16th World Conference on Earthquake, 16WCEE 2017

Santiago Chile, January 9th to 13th 2017

Paper N° 178

Registration Code: S-K1463019596

SEISMIC RESPONSE ANALYSIS OF URBAN HIGHWAY VIADUCTS UNDER MULTIPLE VEHICLES SUBJECTED TO STRONG EARTHQUAKES

L.M. Anggraini[1], S. Borjigin[2], C.W. Kim[3] and K. Sugiura[4]

(1) *Master Course student, Kyoto University, anggraini.marcelina.67z@st.kyoto-u.ac.jp*
(2) *Doctoral Course student, Kyoto University, su.danna.52r@st.kyoto-u.ac.jp*
(3) *Professor, Kyoto University, kim.chulwoo.5u@kyoto-u.ac.jp*
(4) *Professor, Kyoto University, sugiura.kunitomo.4n@kyoto-u.ac.jp*

Abstract

This paper is intended to investigate the effect of vehicles on seismic responses of urban highway viaducts under strong earthquakes. Bridge design codes in most countries do not consider vehicle load in the seismic design because of the low probability of encountering critical vehicle load and earthquake simultaneously. However, considering high probability of traffic jam in urban areas of earthquake prone countries it must be clarified what is the effect of vehicles to seismic responses of bridges. Unfortunately very few researches have noted seismic responses of bridges under traffic during strong earthquakes. Therefore in this study, the vehicles parked on a highway viaduct were considered as dynamic system and were treated as structural members of the bridge model to investigate the effect of vehicles on seismic responses of the viaduct. Validity of the approach that considers vehicles as a part of structural members of the bridge model is verified by comparing with the result from the analysis of vehicle-bridge interaction under strong earthquakes. In the seismic response analysis, three different scenarios were considered to investigate influences of vehicles on the bridge to seismic responses of the bridge under strong earthquakes: i.e. the scenario without considering vehicles; the scenario considering vehicles as additional mass; and finally the scenario considering vehicles as dynamic system. A nonlinear rotational spring was adopted to model the base of bridge piers.

Keywords: finite element model; non-linear seismic response; seismic response analysis; strong earthquake; vehicle load.

1. Introduction

The bridge design code in most countries do not consider the vehicle load and the earthquake load at the same time because of the low probability of simultaneous occurrence of critical vehicle load and a strong earthquake [1]. However, considering the high probability of traffic jam in the urban area of earthquake prone regions such as Japan, there is room for discussion on the effect of vehicle load on the seismic response of the bridge during strong earthquakes.

A study addressing this matter was done by Kameda *et al*. (1999), which concluded that seismic responses of the bridge increase or decrease depending to the phase difference between the bridge and the vehicle [2]. Kim and Kawatani (2006) investigated the effect of train on the linear seismic response of monorail bridges under moderate earthquakes and concluded that the dynamic interaction between the bridge and the train system reduces the seismic response of the bridge compared with the system which consider train as an additional mass [3]. Another study by Kim *et al*. (2011) concluded that the seismic response of the highway bridge increased when the vehicle is considered as mass; and decreased when the vehicle is considered as dynamic system [4].

While some of studies have been done on the linear seismic response analysis, only few studies have been done on the non-linear seismic response analysis. The study by Borjigin *et al*. (2015) examined the effect of moving vehicles on the seismic responses of highway bridges considering both non-linearity and vehicle-bridge interaction although a lot of computational time was needed [5].

This study aims to simulate the effect of stationary vehicles on the seismic responses of highway bridges when subjected to strong earthquakes, which cause nonlinear seismic behaviors of bridges. It is noteworthy that seismic responses under moving vehicles needs to consider the vehicle-bridge interaction (VBI) but for the scenario of stopped vehicles during a strong earthquake it might be an option to model the vehicles as structural members on the bridge if the validity of the idealization is verified.

In this study the validity of modeling the vehicles as structural members on the bridge during strong earthquakes is investigated by comparing with seismic responses from nonlinear seismic analysis considering VBI. This study gives more options for the engineers who would like to analyze seismic behaviors of bridges. Of course an analysis with a higher accuracy can be achieved by considering vehicle-bridge interaction under strong earthquakes, which is yet a challenging research, while a simple preliminary analysis can be achieved by the approach discussed in this study.

2. Analytical Model

ABAQUS/CAE, commercial FE software, was utilized in this study. The stationary vehicles on top of the bridge were treated as structural members of the bridge model. They were represented as mass-spring-damper model and connected to the bridge.

2.1 Vehicle model

A cargo truck was simplified into mass-spring-damper model with two degree of freedoms (in transversal and vertical directions). Table 1 shows the properties of vehicle model in this study, referred to the paper [6] which considered twelve degree of freedoms vehicle model. The mass of vehicle model was lumped on the top of the bridge model. The height of vehicle from the bridge top to its center of mass was considered to be 1.55 m as shown in Fig. 1.

The natural frequency of the vehicle, f_v, can be calculated by Eq. (1).

$$f_v = \frac{1}{2\pi}\sqrt{\frac{k_v}{m_v}} \tag{1}$$

where k_v and m_v are the spring constant and mass of the vehicle, respectively. The natural frequencies of the vehicle in the vertical and transversal directions were 2.75 Hz and 1.54 Hz, respectively.

Table 1 – Properties of vehicle model.

Parameter	Unit	Value
Mass	kg	17,870
Vertical spring constant	N/m	5.33×10^6
Transversal spring constant	N/m	1.67×10^6
Vertical damping coefficient	N.s/m	2.78×10^4
Transversal damping coefficient	N.s/m	2.78×10^4

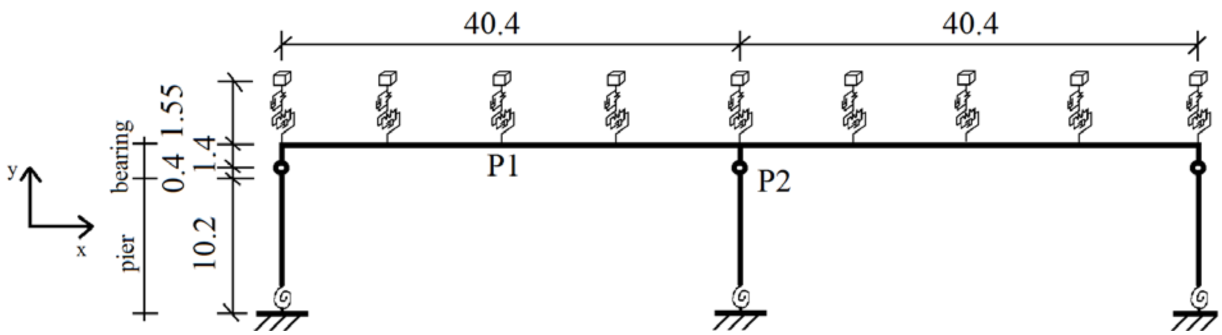

Fig.1 – Bridge and vehicle models. (unit: m)

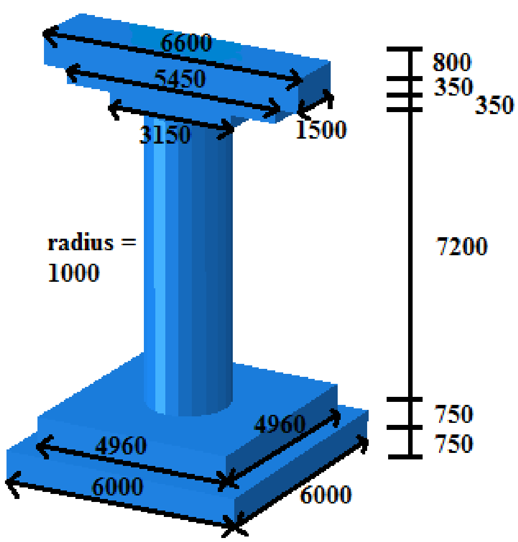

Fig. 2 – Dimension of RC pier. (mm)

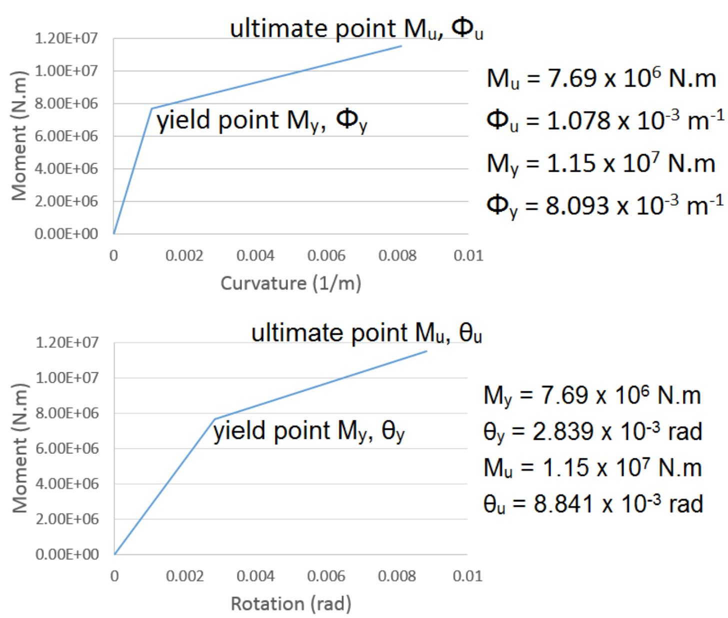

Fig. 3 – Properties of nonlinear rotational spring.

Nine vehicle models that are assumed to stop on the bridge were connected to the bridge and treated as structural members of the bridge. The distance between consecutive vehicles is 10.1 m; the loading configuration is also shown in Fig.1. This vehicle loading pattern, despite unrealistic, was selected to emphasis the effect of vehicles to seismic responses of the bridge.

Table 2 – Properties of bridge material used in the simulation.

Material	Density (kg.m^{-3})	Young's modulus (N.m^{-2})	Poisson's ratio	Rayleigh Damping	
				Alpha	Beta
Steel	3425	2.1×10^{11}	0.2	1.111	0.001415
Concrete	2500	3.0×10^{10}	0.167	0.934	0.000749
Rigid	0	2.1×10^{13}	0	0	0

Table 3 – Natural frequencies and mode shapes of the bridge before yielding.

Transversal mode	Without vehicle	With vehicles as dynamic systems	With vehicles as mass
1st	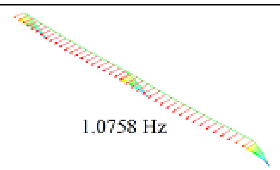	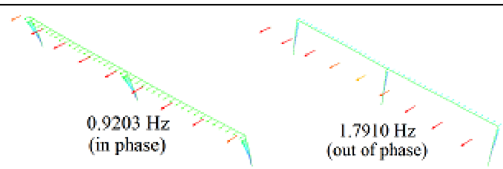	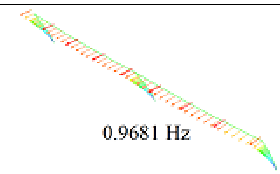
2nd	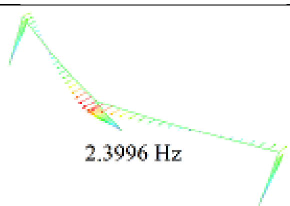	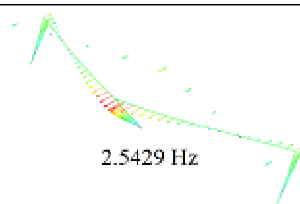	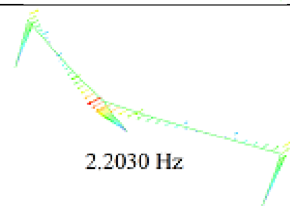
3rd	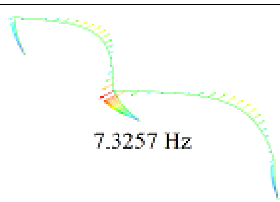	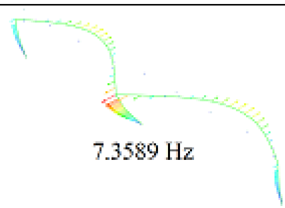	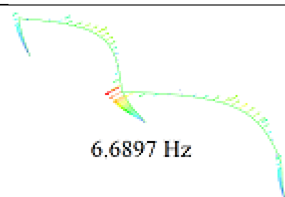

Table 4 – Natural frequencies and mode shapes of the bridge after yielding.

Transversal mode	Without vehicle	With vehicles as dynamic systems	With vehicles as mass
1st	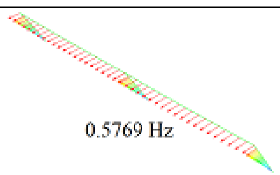	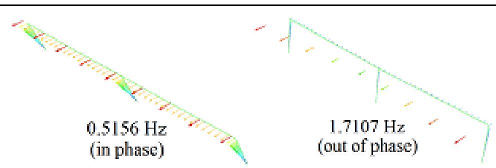	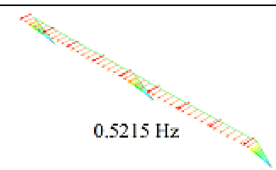
2nd	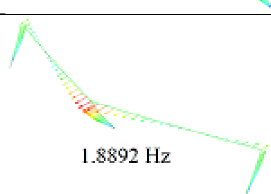	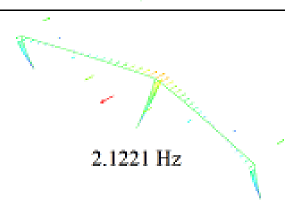	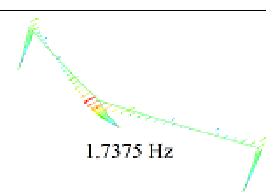
3rd	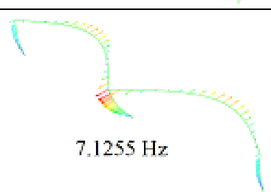	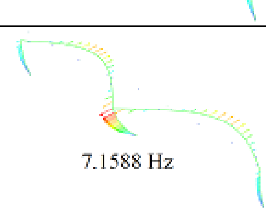	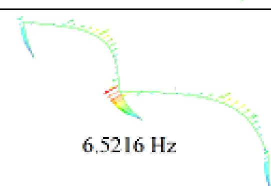

Table 5 – Second moment of inertia, and polar moment of inertia of the bridge model.

	Second moment of area (m^4)			Polar moment of inertia (m^4)	
	I_x	I_y	I_z	J_x	J_y
Girder		0.810	0.203	1.013	
Bearing		0.810	0.203	1.013	
Pier (from top)	35.937		1.856		37.793
	20.235		1.533		21.768
	3.907		0.886		4.793
	0.785		0.785		1.571
	50.437		50.437		100.873
	108.000		108.000		216.000

2.2 Bridge model

The bridge model was a two-span girder bridge of which dimensions are shown in Fig. 1. This bridge model is a part of continuous bridge; the effect of adjacent girder was considered by applying the mass of half girder as point mass on top of the side piers. Two observation points were chosen: P1 at the middle of left girder and P2 at the top of middle pier. The steel girders and RC piers are connected by rigid bearings, and those mechanical properties are summarized in Table 2. The shape of the girder in the real bridge was a truss structure, this study simplified the shape of the girder into a plate, which in turn changed the dimension of the cross-section and therefore the density of the steel material used in the simulation.

The dimension of the simplified pier model is shown in Fig. 2. Table 5 shows the dimension of the cross-section, the second moment of area, and the polar moment of inertia of the bridges. The supports of the girders were modeled as a pin and roller. Each girder was discretized into 20 elements. The FE model of the bridge comprised 134 elements and 413 nodes in total.

The nonlinear behavior of the bridge was assumed to occur at the base of piers and modeled as a nonlinear rotational spring of which properties are shown in Fig. 3. The moment-curvature relationship was transformed into moment-rotation based on Eurocodes [7]. The nonlinear rotational springs rotated along the longitudinal axis. The clockwise angle started from the vertical axis is adopted as the positive angle.

The natural frequencies and mode shapes of the bridge-vehicles system were obtained from the Eigen value analysis and selected ones are shown in Table 3 and Table 4 following those before and after yielding respectively. Due to the different properties of rotational spring before and after yielding, there were two sets of corresponding natural frequencies. In the case of the bridge with vehicles considered as dynamic systems, two transversal modes and frequencies are summarized in the 1st transversal mode: the lower and the higher frequencies correspond with vehicles' in-phase and out-of-phase with the bridge, respectively. The arrows on the mode shapes indicate the direction and the amount of modal deformation; the red with long arrow corresponds with larger deformation than the blue with short arrows.

2.3 Ground motion excitations

Three strong ground motions observed in the 1995 Kobe earthquake were considered as ground motion excitations in this study: JR Takatori Station NS component (hereafter Seismic-1), JR Takatori Station EW component (hereafter Seismic-2), and Osaka Gas Fukiai EW component (hereafter Seismic-3). The time histories of three ground motion excitations are shown in Fig.4, in which the maximum acceleration of Seismic-1 is 6.8683 m/s^2, for the Seismic-2 is 6.7264 m/s^2 and for the Seismic-3 is 7.3633 m/s^2. These data were input ground motions in the transversal direction, with the vertical acceleration assumed to be half of the transversal acceleration. The noted frequencies on the power spectra in Fig.4 are relevant to the 1st transversal mode of each analytical model: 0.92Hz for the bridge with vehicles; 0.97Hz for the bridge with additional mass from vehicles; and 1.08Hz for the bridge without considering vehicles.

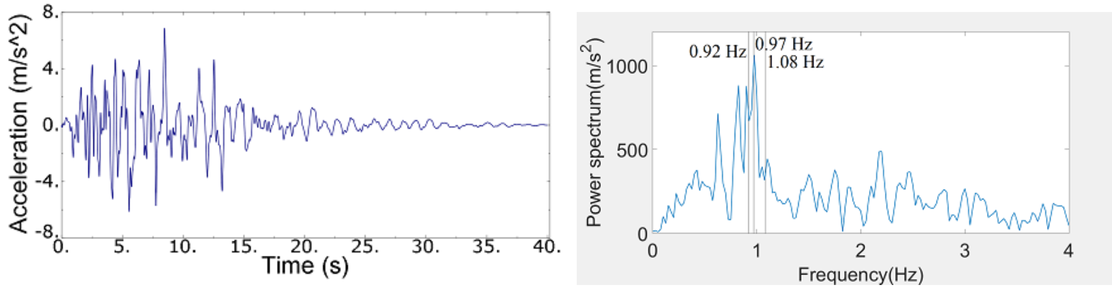

(a) JR Takatori Station NS component (Seismic-1)

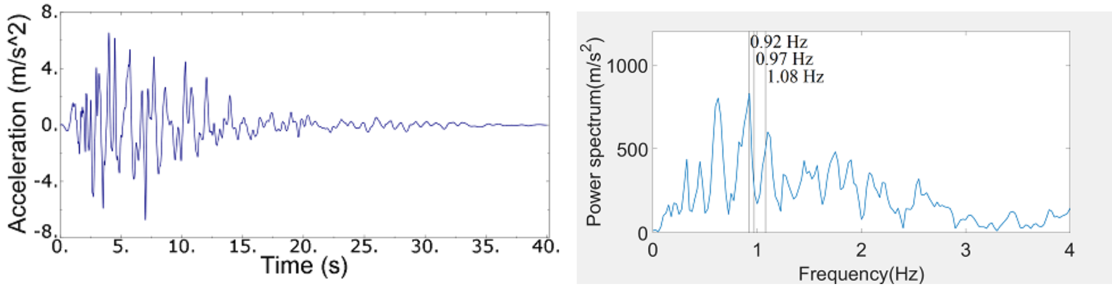

(b) JR Takatori Station EW component (Seismic-2)

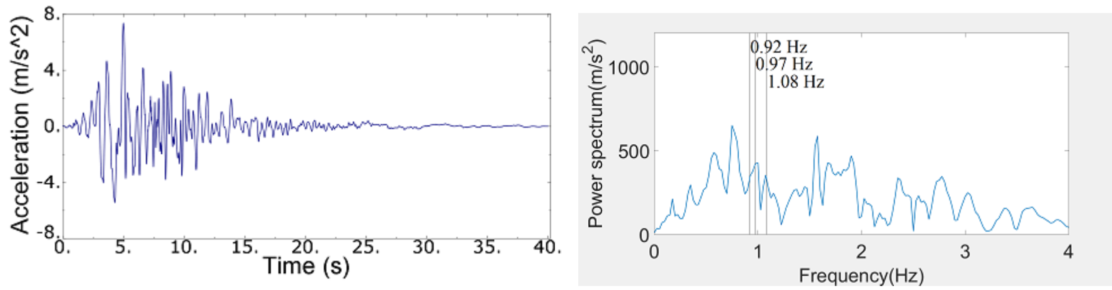

(c) Osaka Gas Fukiai EW component (Seismic-3)

Fig. 4 – Strong ground motions from JRA code.

3. Results and Discussions

3.1 Comparison with VBI system

The analytical results in this study were verified by comparing to the seismic responses of the highway bridge under stationary vehicles that were simulated by means of the partition iteration algorithm considering the VBI [5], which is a more proper way to simulate the bridge and the vehicles but needs more computational time. This study utilizes exactly same properties of the bridge and the vehicles, the configuration of the stationary vehicles, and the seismic data with being considered in [5] that used both ABAQUS and MATLAB. The bridge was simulated in ABAQUS; while the vehicles were simulated in MATLAB. For each time step, the analysis went back and forth from one software to another; which is why a lot of computational time was needed to finish the simulation.

The transversal displacements of bridge with vehicles under Seismic-1 in this study were compared with those of the VBI model to examine feasibility of the simplified approach proposed in this study, and shown in Fig. 5. The numerical values of the maximum displacement, permanent displacement, and the differences are shown in Table 6.

As shown in Table 6, the model in this study gave underestimated results in the maximum and permanent transversal displacement compared with the VBI model. In average, the differences were 2.12% in the maximum displacement and 4.97% in the permanent transversal displacement, respectively. One of the possible reasons for this difference is the different loading condition (Fig. 6) of the vehicle models. In this study, the vehicle model was connected to a node of the bridge model, and therefore the mass was modeled as concentrated load; while in the VBI model, the weight of the vehicle was modeled as distributed load with 1m in length. The VBI model also covers the case of moving vehicles, this distributed load was chosen to ensure that the vehicle load always comes into contact with the integration points in the bridge model, else ABAQUS cannot detect the vehicle load.

The model in this study gave comparable results with the VBI model, which means that a simpler preliminary analysis can be done by the approach in this study.

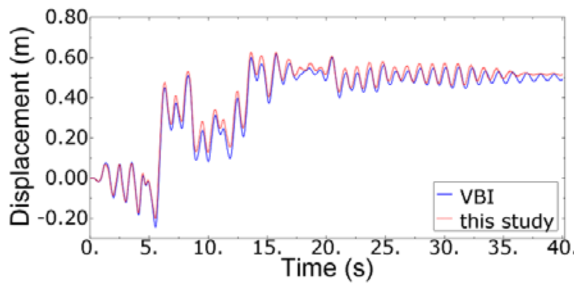

Fig. 5 – The transversal displacement at P2 of bridge with vehicles under Seismic-1 in this study and VBI model.

Table 6 – The difference of displacements between this study and analysis considering VBI.

	VBI model		This study	
	At P1	At P2	At P1	At P2
Maximum displacement (m)	0.709	0.618	0.729	0.627
Difference in maximum displacement (%)	-	-	2.81	1.43
Permanent displacement (m)	0.576	0.492	0.606	0.515
Difference in permanent displacement (%)	-	-	5.20	4.73

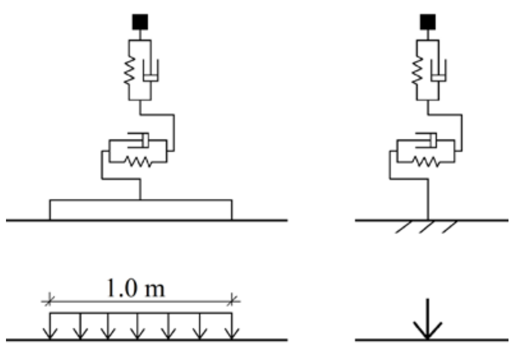

Fig.6 – Loading condition in VBI model (left) and in this study (right).

3.2 Transversal displacements

Fig. 6 shows the time histories of transversal displacements at P2 of the bridge without vehicle, with vehicles, and with vehicles as mass and the hysteresis curves at the base of middle pier when subjected to strong earthquakes. The time histories of transversal displacement of the bridge at P1 showed the same trend as those at P2. Three cases were considered: bridge without any vehicle, bridge with nine vehicles as dynamic systems, and bridge with nine vehicles as mass. Although the second case is more realistic, the third case was simulated and compared in order to understand the effect of springs and dampers on the vehicle models.

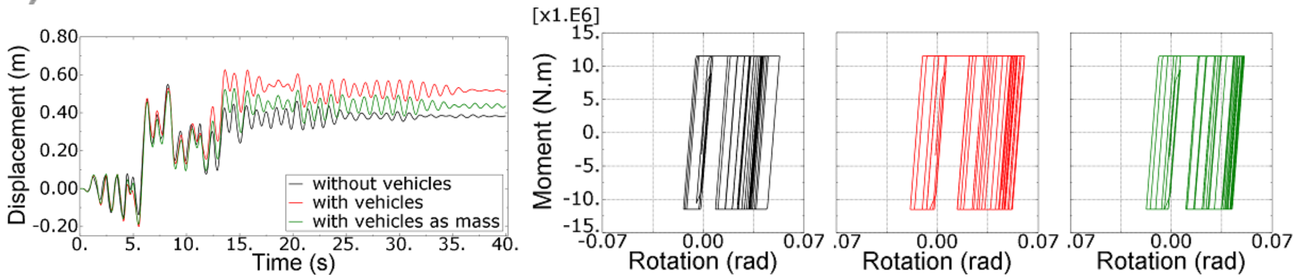

(a) Under Seismic-1

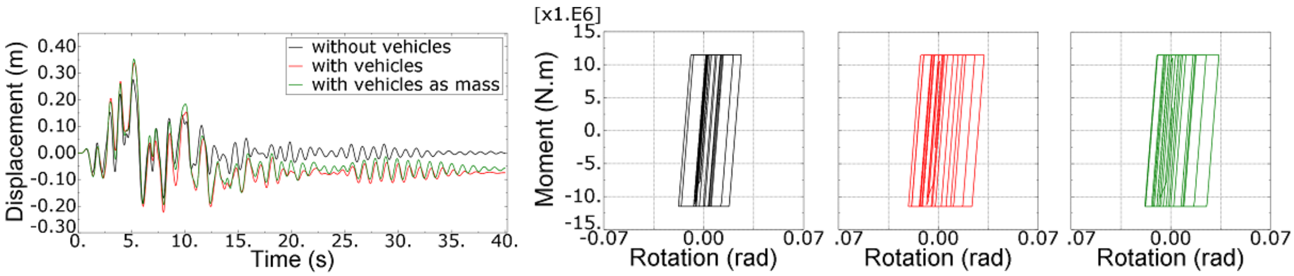

(b) Under Seismic-2

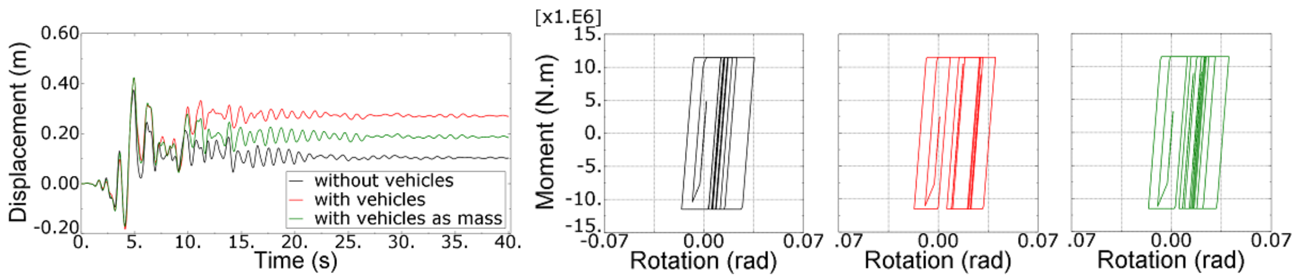

(c) Under Seismic-3

Fig. 6 - The transversal displacements at P2 of bridge without vehicle, with vehicles, and with vehicles as mass and the hysteresis curves at the base of middle pier.

The hysteresis curves at the bottom of middle piers when subjected to strong earthquakes are also shown in Fig. 6. The maximum angle in the hysteresis curve correlates with the maximum transversal displacement. Under the Seismic-1, the maximum angle in the hysteresis curve of the bridge with vehicles as dynamic systems was larger than those as mass, which also larger than those without vehicle; the same trend can be seen in the maximum transversal displacement of the bridge under the Seismic-1. Under Seismic-2 and Seismic-3, the maximum angle in the hysteresis curve of the bridge with vehicles as mass was larger than that considering vehicles as dynamic systems, which was also larger than that without vehicles; the same trend can be seen in the maximum transversal displacement of the bridge under Seismic-2 and Seismic-3.

Maximum displacements at the observation points P1 and P2 of the bridge are summarized in Table 7 with the average increment of the maximum displacement from the scenario of without considering vehicles. The permanent and averaged displacements at P2 are shown in Table 8. JRA (Japan Road Association) specified the allowable permanent displacement at the observed pier top (P2 in this study) as 1/100 of the distance between pier bottom and the gravity center of the girder as shown in Eq.(2) [8].

$$\delta_R \leq \delta_{Ra}\left(= H/100\right) \tag{2}$$

where, δ_R is the average residual displacement; δ_{Ra} indicates the allowable residual displacement; H is the distance in meter between the pier base and the neutral axis of the girder.

For the bridge model used in this study, the allowable permanent displacement is 0.120 m. Averaging the responses in the observation point P2, the permanent displacement for all scenarios were larger than the allowable permanent displacement; 0.163 m, 0.286 m, and 0.225 m for bridge without vehicles, with vehicles, and with vehicles as mass, respectively. It is noteworthy that the bridge was designed and built before the Kobe earthquake although the allowable permanent displacement in Eq. (2) is specified after the Kobe earthquake.

Under each of the three ground motions used in this study, the existence of vehicles (either as dynamic systems or as mass) raised the transversal displacement of the bridge, except one case: the scenario considering vehicles as mass resulted in decrease of the maximum displacements under the Seismic-1. When the effect of addition of vehicles as dynamic systems and as mass were compared, vehicles as dynamic systems showed larger permanent displacement than vehicles as mass. When the average displacements under three ground motions were compared, the existence of vehicles (either as dynamic systems or as mass) raised the transversal displacement of bridge, and larger effect was observed by considering vehicles as dynamic systems.

Table 7 – Maximum transversal displacement of bridge without vehicle, with vehicles, and with vehicles as mass under all earthquakes at all observation points. (unit: m)

		at P1	Average increment at P1 from the scenario of W/O vehicles	at P2	Average increment at P2 from the scenario of W/O vehicles
W/O vehicles	Seismic-1	0.638	-	0.549	-
	Seismic-2	0.315	-	0.276	-
	Seismic-3	0.448	-	0.376	-
W/vehicles	Seismic-1	0.729	0.092 (14.4%)	0.627	0.077 (14.0%)
	Seismic-2	0.401	0.086 (27.4%)	0.339	0.062 (22.5 %)
	Seismic-3	0.512	0.064 (14.3%)	0.423	0.049 (13.0%)
W/vehicles as mass	Seismic-1	0.614	-0.024 (-3.8%)	0.528	-0.022 (-3.9%)
	Seismic-2	0.404	0.089 (28.2%)	0.352	0.076 (27.6%)
	Seismic-3	0.507	0.059 (13.1%)	0.424	0.050 (13.3%)

Table 8 – Permanent transversal displacement (absolute) of bridge without vehicle, with vehicles, and with vehicles as mass under all earthquakes at all observation points. (unit: m)

		at P2	Average increment at P2 from the scenario of W/O vehicles	Average displacement at P2
W/O vehicles	Seismic-1	0.383	-	0.163
	Seismic-2	0.002	-	
	Seismic-3	0.103	-	
W/vehicles	Seismic-1	0.515	0.133 (34.7%)	0.286
	Seismic-2	0.074	0.073 (4169.1%)	
	Seismic-3	0.269	0.166 (161.9%)	
W/vehicles as mass	Seismic-1	0.436	0.052 (13.9%)	0.225
	Seismic-2	0.056	0.054 (3091.1%)	
	Seismic-3	0.184	0.082 (79.4%)	

(a)
(b)
(c)
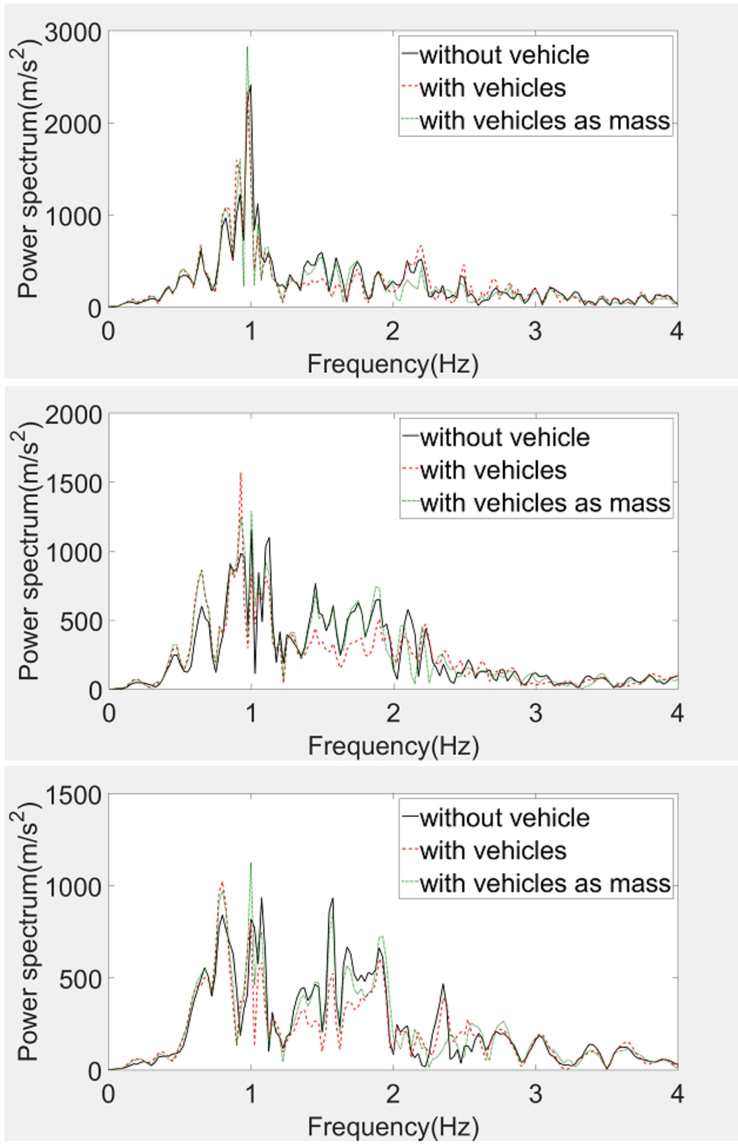

Fig. 11 – The power spectra of transversal acceleration of the bridge without vehicles, with vehicles, with vehicles as mass at P2 under: (a) Seismic-1; (b) Seismic-2; (c) Seismic-3.

3.3 Transversal accelerations

How vehicles affect the transversal acceleration of the bridge under the strong earthquakes is examined focusing on changes in dominant frequencies. The power spectra of transversal acceleration of the bridge at the observation point P2 under three strong earthquakes are shown in Fig. 11.

Fig. 11 (a) shows the power spectra of transversal acceleration of the bridge at the observation point P2 under the Seismic-1. The peak at 0.975 Hz was greatly influenced by the earthquake; the highest peak of the power spectrum of Seismic-1 is 0.975 Hz as shown in Fig. 4(a). This peak also corresponded with the first transversal mode of the bridge with vehicles as mass (0.97 Hz), which in response caused the power spectrum of the bridge with vehicles as mass to be larger than those of the bridge with vehicles and without vehicles.

Fig. 11(b) shows the power spectra of transversal acceleration of the bridge at the observation point P2 under the Seismic-2. The shift of peaks around 1 Hz was caused by the shift of frequency of the first transversal mode. The highest peak of response of the bridge with vehicles at 0.925 Hz corresponded with the frequency of the first transversal mode of bridge with vehicles, 0.92 Hz. The highest peak of response of the bridge with vehicles as mass at 1.00 Hz corresponded with the frequency of the first transversal mode of bridge with vehicles as mass, 0.97 Hz. The peak at 1.125 Hz on the power spectrum of the acceleration of the bridge without vehicles corresponds with the frequency of the first transversal mode of bridge without vehicle, 1.08 Hz.

Fig. 11(c) shows the power spectra of transversal acceleration of the bridge at observation point P2 under the Seismic-3. Four peaks were observed. First, for the peak at 0.80 Hz which is influenced by the highest peak in the Seismic-3 (0.75 Hz) as shown in Fig. 4(c), the power spectra of the bridge with vehicles were larger than those of the bridge with vehicles as mass, and both of them were larger than those of the bridge without vehicle. Second and third, the peak at 1.00 Hz and 1.075 Hz; the powers of the Seismic-3 associated with these peaks were relatively small, but the power spectra of the bridge responses were large due to resonance with the frequency of the first transversal mode of the bridge. Fourth, for the peak at 1.575 Hz that is relevant to the second highest peak in the Seismic-3, the power spectra of the bridge without vehicles were larger than those of the bridge with vehicles as mass. It is noteworthy that the power at 1.575 Hz of the bridge with vehicles as dynamic systems was smaller than that of scenarios without vehicles and vehicles as mass. One reason for this result can be explained utilizing the mode shapes in Tables 3 and 4 that the model considering vehicles have out-of-phase mode between the bridge and vehicles at 1.79Hz before yielding and 1.71Hz after yielding may reduce the seismic responses relevant to 1.575 Hz.

4. Conclusions

This study investigated the effect of stationary vehicles on the non-linear seismic response of highway bridges. ABAQUS was utilized to simulate the model. The simplified model in this study gave comparable results with those considering a VBI model, which means that this method can be used for a preliminary analysis. Considering vehicles (either as dynamic systems or as mass) changed the frequency characteristic of the bridge, and thus resulting different seismic responses. Averaging the response under the three earthquakes used in this study, addition of vehicles raised the seismic response of the bridge, with larger increment in permanent displacement caused by vehicles as dynamic systems.

The next step for this study could be to investigate different bridge and vehicle models, for example longer span bridge with steel piers, and to consider slipping of the vehicles, to derive more general conclusions on the influence of vehicles on the nonlinear seismic responses of the highway bridge.

5. References

[1] Wibowo H, Sanford DM, Buckle IG, Sanders DH (2012): Effects of live load on seismic response of bridges: a preliminary study. *Civil Engineering Dimension,* 14 (3), pp. 166-172. doi: 10.9744/ced.14.3.166-172.

[2] Kameda H, Murono Y, Nanjou A, Sasaki N (1999): Earthquake response of highway bridges under bridge-vehicle system. *J. of Struct. Mech. Earthquake Eng., JSCE*, 626(I-48), 93-106.

[3] Kim CW, Kawatani M (2006): Effect of train dynamics on seismic response of steel monorail bridges under moderate ground motion. *Earthquake Engineering and Structural Dynamics*, **35** (10), 1225-1245. doi: 10.1002/eqe.580.

[4] Kim CW, Kawatani M, Konaka S, Kitaura R (2011): Seismic responses of a highway viaduct considering vehicles of design live load as dynamic system during moderate earthquakes. *Structure and Infrastructure Engineering*. Vol.7, No.7-8, pp.523-534.

[5] Borjigin S, Kim CW, Chang KC and Sugiura K (2015): Non-linear seismic response analysis of vehicle-bridge interactive systems. *Steel Construction*, 8: 2–8. doi: 10.1002/stco.201510006.

[6] Kawatani M, Kim CW, Iwashita K and Yasui K (2008): *Seismic responses of highway viaducts incorporating bridge-vehicle interaction*. *Doboku Gakkai Ronbunshuu A* (*J. of Struct. Mech. Earthquake Eng, A*), JSCE, 64(4), pp.678-691.

[7] CEN (2005): *European Standard EN 1998-2, Eurocode 8: Design of structures for earthquake resistance: Bridges*, 132-134. Retrieved from: https://law.resource.org/pub/eu/eurocode/en.1998.2.2005.pdf

[8] Japan Society of Civil Engineers (2000): *Earthquake resistant design codes in Japan*, JSCE, Tokyo, Japan. ISBN: 4-8106-0266-4.